



(19) **United States**

(12) **Patent Application Publication**

Jung et al.

(10) **Pub. No.: US 2024/0145672 A1**

(43) **Pub. Date: May 2, 2024**

(54) **POSITIVE ELECTRODE ACTIVE MATERIAL, POSITIVE ELECTRODE INCLUDING THE SAME, AND LITHIUM SECONDARY BATTERY**

Publication Classification

- (51) **Int. Cl.**
H01M 4/36 (2006.01)
H01M 4/505 (2006.01)
H01M 4/525 (2006.01)
H01M 10/052 (2006.01)
- (52) **U.S. Cl.**
 CPC *H01M 4/362* (2013.01); *H01M 4/505* (2013.01); *H01M 4/525* (2013.01); *H01M 10/052* (2013.01); *H01M 2004/028* (2013.01)

(71) Applicant: **LG Chem, Ltd.**, Seoul (KR)

(72) Inventors: **Won Sig Jung**, Daejeon (KR); **Hwan Young Choi**, Daejeon (KR); **Jong Pil Kim**, Daejeon (KR); **Yeo June Yoon**, Daejeon (KR); **Kang Hyeon Lee**, Daejeon (KR); **Tae Young Rhee**, Daejeon (KR); **Yong Jo Jung**, Daejeon (KR)

(57) **ABSTRACT**

Provided is a positive electrode active material which includes an inner region that is a region from the center of the positive electrode active material particle to R/2, and an outer region that is a region from R/2 to the surface of the positive electrode active material particle, wherein R is a distance from the center of the positive electrode active material particle to the surface thereof. The positive electrode active material further includes 25% to 80% of crystallites C with respect to a total number of crystallites in the outer region. The crystallites C have a high crystallite long-axis orientation degree of 0.5 to 1 and a low crystallite c-axis orientation degree less than 0.5. Thus, the positive electrode active material has high capacity characteristics and a small amount of gas generated.

(73) Assignee: **LG Chem, Ltd.**, Seoul (KR)

(21) Appl. No.: **18/278,321**

(22) PCT Filed: **Mar. 22, 2022**

(86) PCT No.: **PCT/KR2022/003974**

§ 371 (c)(1),

(2) Date: **Aug. 22, 2023**

(30) **Foreign Application Priority Data**

Mar. 22, 2021 (KR) 10-2021-0036942

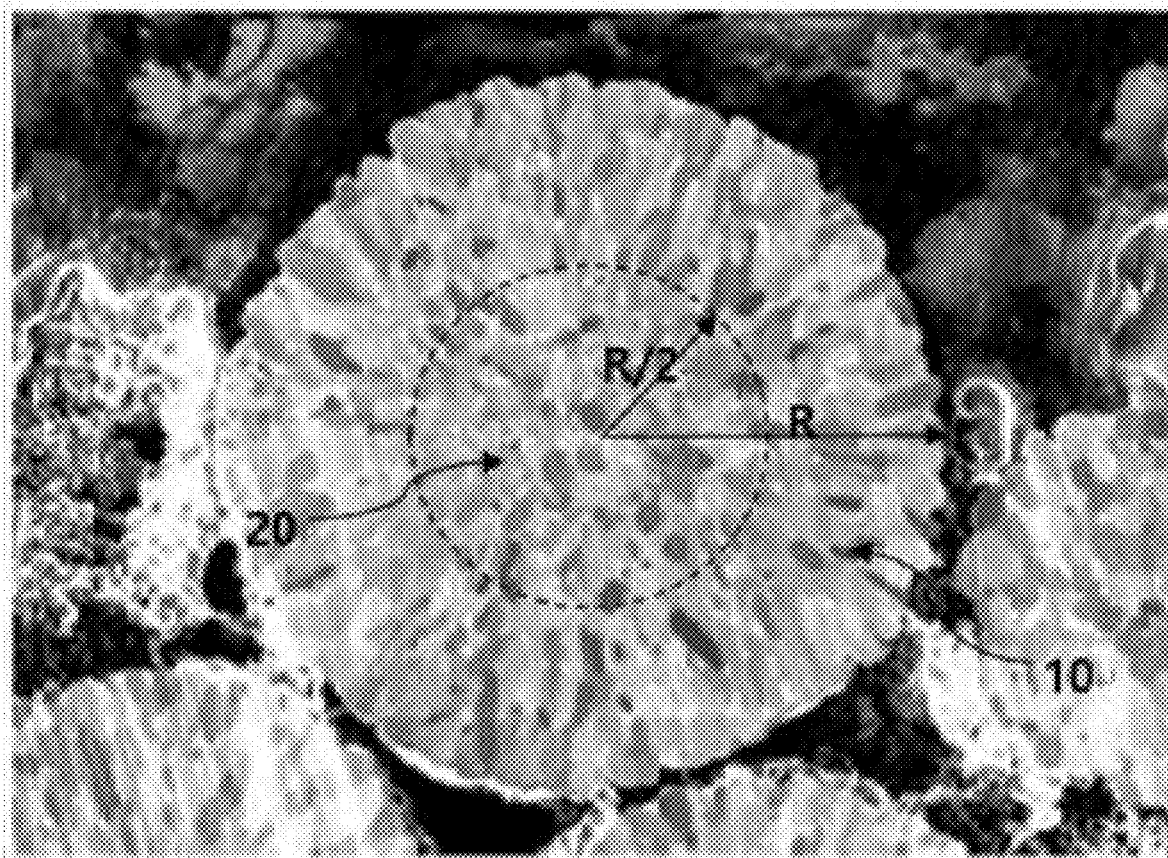


[FIG. 1]

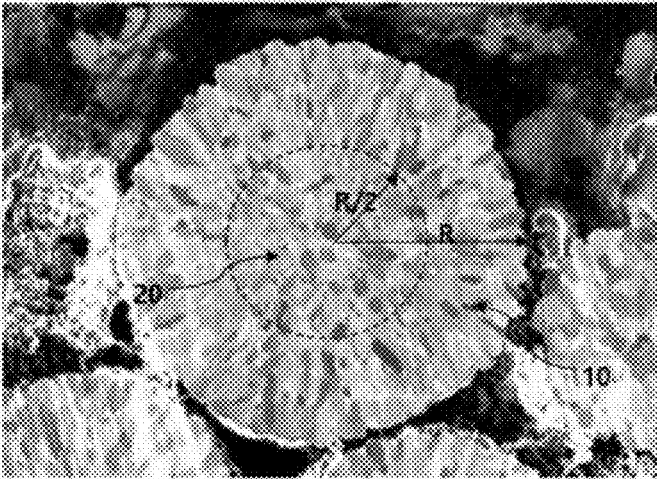
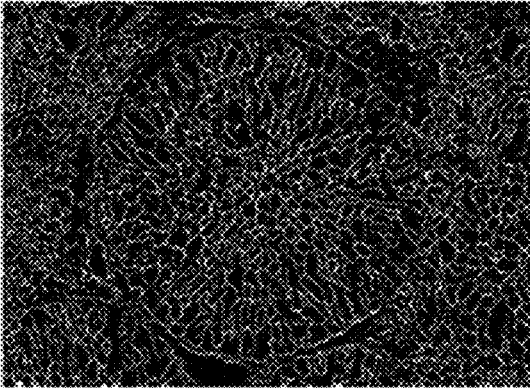


[FIG. 2]

DL Boundary detection



ML segmentation

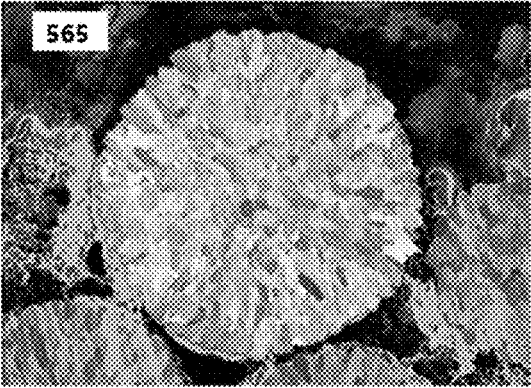


[FIG. 3]

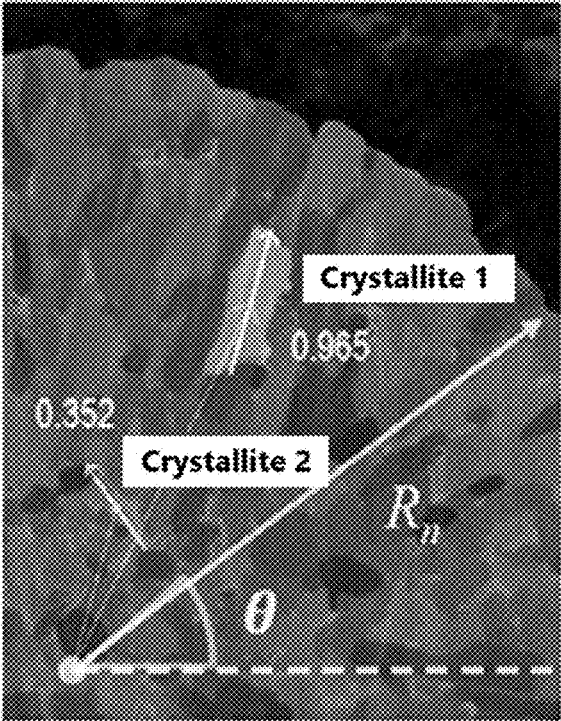


[FIG. 4]

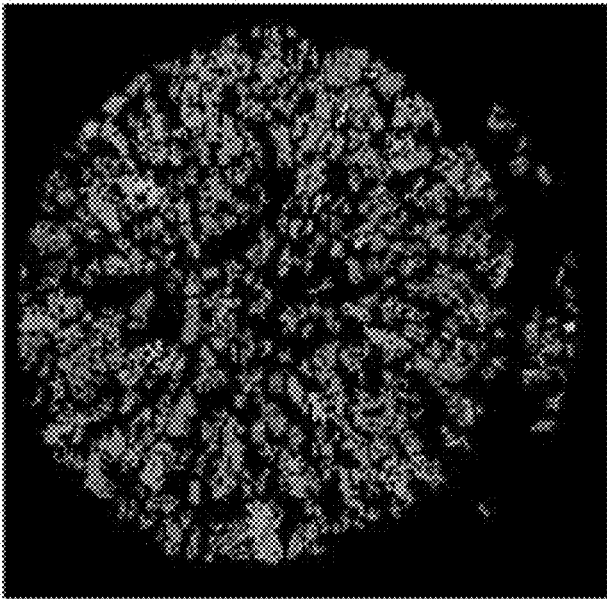
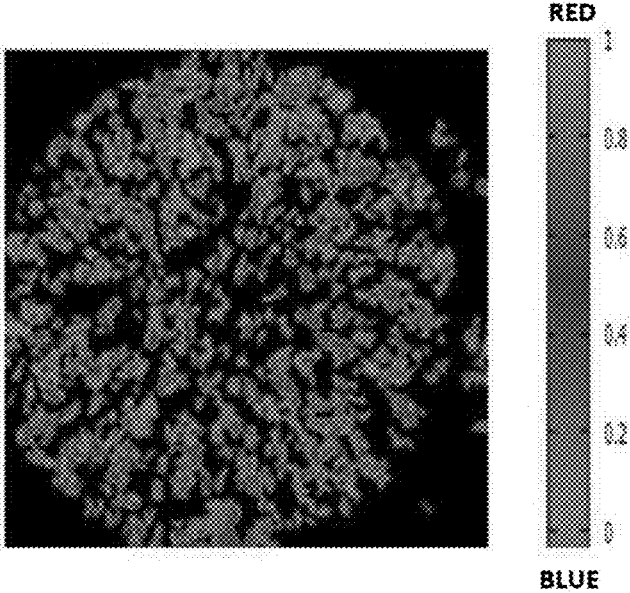


[FIG. 5]



**POSITIVE ELECTRODE ACTIVE
MATERIAL, POSITIVE ELECTRODE
INCLUDING THE SAME, AND LITHIUM
SECONDARY BATTERY**

**CROSS-REFERENCE TO RELATED
APPLICATIONS**

[0001] This application is a national phase entry under 35 U.S.C. § 371 of International Application No. PCT/KR2022/003974, filed on Mar. 22, 2022, which claims the benefit of Korean Patent Application No. 10-2021-0036942, filed on Mar. 22, 2021, the disclosures of which are incorporated herein in their entireties by reference.

TECHNICAL FIELD

[0002] The present invention relates to a positive electrode active material, a positive electrode including the same, and a lithium secondary battery, and more particularly, to a positive electrode active material for a lithium secondary battery having excellent capacity characteristics and generating less gas, a positive electrode including the same, and a lithium secondary battery.

BACKGROUND ART

[0003] Demand for secondary batteries as an energy source has been significantly increased as technology development and demand with respect to mobile devices and electric vehicles have recently increased. Among these secondary batteries, lithium secondary batteries having high energy density, high voltage, long cycle life, and low self-discharging rate have been commercialized and widely used.

[0004] Lithium transition metal oxides, such as lithium cobalt oxides such as LiCoO_2 , lithium nickel oxides such as LiNiO_2 , lithium manganese oxides such as LiMnO_2 or LiMn_2O_4 , or lithium iron phosphates such as LiFePO_4 , have been developed as a positive electrode active material of the lithium secondary battery, and, recently, lithium composite transition metal oxides including two or more types of transition metals, for example, $\text{Li}[\text{Ni}_a\text{Co}_b\text{Mn}_c]\text{O}_2$, $\text{Li}[\text{Ni}_a\text{Co}_b\text{Al}_c]\text{O}_2$, and $\text{Li}[\text{Ni}_a\text{Co}_b\text{Mn}_c\text{Al}_d]\text{O}_2$, have been developed and widely used.

[0005] Lithium composite transition metal oxides including two or more transition metals which have been developed so far are generally prepared in the form of spherical secondary particles in which dozens to hundreds of primary particles are aggregated. Physical properties such as mobility of lithium ions or impregnation of an electrolyte may vary depending on the orientation of the primary particles or the shape (aspect ratio) of the primary particles. Accordingly, studies to improve the performance of positive electrode active materials by controlling the particle structure of positive electrode active material particles have been attempted.

[0006] Korean Patent No. 10-1611784 (Patent Document 1) discloses a positive electrode active material in which the length of an a-axis direction of a primary particle is longer than the length of a c-axis direction, and the a-axis of the primary particle is radially arranged. In Patent Document 1, the shape of the primary particles or the orientation of the primary particles of the positive electrode active material was analyzed using a scanning electron microscope (SEM) and/or a transmission electron microscope (TEM).

[0007] However, the TEM analysis used in Patent Document 1 has a problem in that it is difficult to represent the properties of the entire positive electrode active material particles because only information on a partial region rather than the entirety of the particles may be obtained. In addition, since the physical properties of the positive electrode active material vary depending on the shape or orientation of the crystallites as well as the shape or orientation of the primary particles, the positive electrode active material may exhibit different physical properties even when the shape or orientation of the primary particles is similar.

[0008] Therefore, in order to develop a positive electrode active material having better properties, studies on a crystallite structure of the positive electrode active material are required.

Technical Problem

[0009] An aspect of the present invention provides a positive electrode active material which has excellent capacity characteristics and generates less gas by including, in a particular proportion, crystallites in which the orientation of the long-axis and the c-axis of the crystallite in the outer region of the positive electrode active material particle satisfies a particular condition.

[0010] Another aspect of the present invention provides a positive electrode and a lithium secondary battery which includes the positive electrode active material according to the present invention.

Technical Solution

[0011] According to an aspect of the present invention, there is provided a positive electrode active material including: an inner region that is a region from a center of a positive electrode active material particle to $R/2$; and an outer region that is a region from $R/2$ to a surface of the positive electrode active material particle, wherein R is a distance from the center of a positive electrode active material particle to the surface thereof, wherein a proportion (C_1) of a plurality of crystallites C is 25% to 80%, preferably 30% to 60%, more preferably 30% to 50%, and even more preferably 30% to 40% with respect to a total number of crystallites in the outer region, wherein a crystallite long-axis orientation degree DoA represented by Equation 1 below is 0.5 to 1, and wherein a crystallite c-axis orientation degree represented by a cross product value of a c-axis rotation vector R_c of a crystal lattice of a crystallite obtained by electron backscatter diffraction (EBSD) analysis and a position unit vector P' of the crystallite is less than 0.5:

$$DoA = \frac{\lambda_1}{\lambda_1 + \lambda_2} C_D^2 \quad \text{[Equation 1]}$$

[0012] In Equation 1 above, λ_1 is a size of a long-axis vector E_l of the crystallite determined from image data obtained by a scanning ion microscope analysis of a cross-section of the positive electrode active material, λ_2 is a size of a short-axis vector E_s of the crystallite determined from image data obtained by the scanning ion microscope analysis of the cross-section of the positive electrode active material, and C_D above is an inner product value of a position unit vector P' and a long-axis vector E_l' of the crystallite.

[0013] The positive electrode active material according to the present invention may have the proportion (C1) of the plurality of crystallites C to the total number of crystallites in the outer region larger than a proportion (C2) of the plurality of crystallites C to a total number of crystallites in the inner region. Specifically, the difference between the proportion (C1) of the plurality of crystallites C to the total number of crystallites in the outer region and the proportion (C2) of the plurality of crystallites C to the total number of crystallites in the inner region may be at least 3%, at least 5%, 3% to 20%, or 3% to 15%.

[0014] Meanwhile, the positive electrode active material may further include a plurality of crystallites A wherein a crystallite long-axis orientation degree DoA is 0.5 to 1 and a crystallite c-axis orientation degree is 0.5 to 1, a plurality of crystallites B wherein a crystallite long-axis orientation degree DoA is less than 0.5 and a crystallite c-axis orientation degree is 0.5 to 1, and a plurality of crystallites D wherein a crystallite long-axis orientation degree DoA is less than 0.5 and a crystallite c-axis orientation degree is less than 0.5.

[0015] In this case, the proportion (C1) of the plurality of crystallites C to the total number of crystallites in the outer region may be larger than each of a proportion (A1) of the plurality of crystallites A, a proportion (B1) of the plurality of crystallites B, and a proportion (D1) of the plurality of crystallites D.

[0016] In addition, a proportion of the plurality of crystallites A to the total number of crystallites in the cross-section of the positive electrode active material may be 5% to 40%, preferably, 10% to 30%, a proportion of the plurality of crystallites B may be 5% to 40%, preferably, 5% to 30%, a proportion of the plurality of crystallites C may be 20% to 80%, preferably, 25% to 60%, and a proportion of the plurality of crystallites D may be 5% to 40%, preferably, 10% to 30%.

[0017] Meanwhile, the scanning ion microscope analysis may be performed by obtaining a scanning ion microscope image by irradiating the cross-section of the positive electrode active material with a focused ion beam, then obtaining data segmented in a crystallite unit from the scanning ion microscope image using deep learning, and calculating DoA represented by Equation 1 above from the segmented data.

[0018] In addition, the EBSD analysis may be performed by obtaining EBSD Euler map data including position information and Euler angle information on each crystallite through EBSD measurement of the cross-section of the positive electrode active material, and calculating the c-axis rotation vector Rc (x, y, z) of the crystal lattice of the crystallite by means of Equation 2 below:

$$\begin{bmatrix} x \\ y \\ z \end{bmatrix} = R_z(\Psi)R_y(\Theta)R_x(\Phi) \begin{bmatrix} X \\ Y \\ Z \end{bmatrix} = \begin{bmatrix} \cos\Psi & -\sin\Psi & 0 \\ \sin\Psi & \cos\Psi & 0 \\ 0 & 0 & 1 \end{bmatrix} \begin{bmatrix} \cos\Theta & 0 & \sin\Theta \\ 0 & 1 & 0 \\ -\sin\Theta & 0 & \cos\Theta \end{bmatrix} \begin{bmatrix} 1 & 0 & 0 \\ 0 & \cos\Phi & -\sin\Phi \\ 0 & \sin\Phi & \cos\Phi \end{bmatrix} \begin{bmatrix} X \\ Y \\ Z \end{bmatrix} = \begin{bmatrix} \cos\Theta\cos\Psi & -\cos\Theta\sin\Psi + \sin\Phi\sin\Theta\cos\Psi & \sin\Phi\sin\Psi + \cos\Phi\sin\Theta\cos\Psi \\ \cos\Theta\sin\Psi & \cos\Phi\cos\Psi + \sin\Phi\sin\Theta\sin\Psi & -\sin\Phi\cos\Psi + \cos\Phi\sin\Theta\sin\Psi \\ -\sin\Theta & \sin\Phi\cos\Theta & \cos\Phi\cos\Theta \end{bmatrix} \begin{bmatrix} X \\ Y \\ Z \end{bmatrix}$$

[0019] In Equation 2 above, [X, Y, Z] is (0, 0, 1), and Φ , Θ , and Ψ each represent an Euler angle obtained from the Euler map data.

[0020] The positive electrode active material according to the present invention may be a lithium composite transition metal oxide represented by Formula 1 below:



[0021] In Formula 1 above,

[0022] M^1 is at least one element selected from the group consisting of Mn and Al, M^2 is at least one element selected from the group consisting of W, Cu, Fe, V, Cr, Ti, Zr, Zn, Al, Ta, Y, In, La, Sr, Ga, Sc, Gd, Sm, Ca, Ce, Nb, Mg, B, and Mo, and A is at least one element selected from the group consisting of F, Cl, Br, I, At, and S, and $0.98 \leq x \leq 1.20$, $0 < a < 1$, $0 < b < 1$, $0 < c < 1$, $0 \leq d \leq 0.2$, $0 \leq y \leq 0.2$.

[0023] According to another aspect of the present invention, there is provided a positive electrode including the positive electrode active material according to the present invention, and a lithium secondary battery including the positive electrode.

Advantageous Effects

[0024] The positive electrode active material of the present invention includes, in a particular proportion, crystallites having high long-axis orientation and low c-axis orientation thereof in an outer region, and thus may have excellent capacity characteristics and generate less gas when applied to a secondary battery. Specifically, Li ions inside the crystallites move along the plane direction of an ab-plane of the crystallite. In the case of the crystallites having low c-axis orientation, contact of an electrolyte and the plane direction of the ab-plane, which is a lithium movement path inside the crystallites, is low, and thus an amount of gas generated due to a side reaction with the electrolyte solution may be reduced. Meanwhile, the Li ions move along the interface between the crystallite and the crystallite after the Li ions are deintercalated from the crystallites. Therefore, when many crystallites having excellent long-axis orientation, in which the long-axis of crystallite is arranged in the direction from the particle center to the surface, are distributed on the surface of the positive electrode active material, the lithium movement path is shortened, and thus lithium mobility may be improved, thereby achieving an effect of improving capacity characteristics. Thus, as in the present invention, when crystallites having high long-axis orientation and low c-axis orientation are contained in high pro-

[Equation 2]

portion in the outer region, an effect of improving both capacity characteristics and gas generation characteristics may be achieved.

BRIEF DESCRIPTION OF THE DRAWINGS

[0025] FIG. 1 is a view showing a scanning ion microscope image of the cross-section of a positive electrode active material;

[0026] FIG. 2 is a view showing a process of obtaining a segmentation image by analyzing a scanning ion microscope image of the cross-section of a positive electrode active material;

[0027] FIG. 3 is a view showing long-axis orientation and DoA values of crystallites;

[0028] FIG. 4 is a view showing an electron backscatter diffraction (EBSD) Euler map obtained by performing EBSD analysis on the cross-section of the positive electrode active material; and

[0029] FIG. 5 is a view showing a c-axis orientation map of crystallites.

DETAILED DESCRIPTION

[0030] It will be understood that words or terms used in the specification and claims shall not be interpreted as the meaning defined in commonly used dictionaries, and it will be further understood that the words or terms should be interpreted as having a meaning that is consistent with their meaning in the context of the relevant art and the technical idea of the invention, based on the principle that an inventor may properly define the meaning of the words or terms to best explain the invention.

[0031] In the present invention, the term “crystallite” refers to a single crystal particle unit having a regular atom arrangement. The size of the crystallite may be measured by analyzing, in the Rietveld refinement method, X-ray diffraction data of the cross-section of positive electrode active material. For example, the crystallite size may be obtained by performing X-ray diffraction analysis under the following conditions using Empyrean XRD equipment from Malver Panalytical, Ltd. to obtain XRD data, and then processing the XRD data using Highscore program from Malver Panalytical, Ltd. In this case, a full width at half maximum is set to be measured using Caglioti equation.

[0032] <X-Ray Diffraction Analysis Conditions>

[0033] Light source: Cu-target, 45 kV, 40 mA output, wavelength=1.54 Å

[0034] Detector: GaliPIX3D

[0035] Sample preparation: About 5 g of a sample is filled in a holder having a diameter of 2 cm and loaded on a rotation stage.

[0036] Measurement time: about 30 minutes

[0037] Measurement region: $2\theta=15^\circ$ to 85°

[0038] In the present invention, the term “primary particle” refers to a minimum particle unit distinguished as a single lump when the cross-section of the positive electrode active material is observed through a scanning electron microscope (SEM), and may be composed of a single crystallite or a plurality of crystallites. In the present invention, an average particle diameter of the primary particles may be determined by a method of measuring each particle size distinguished from cross-sectional SEM data of the positive electrode active material particles and then calculating an arithmetic average value thereof.

[0039] In the present invention, the term “secondary particle” refers to a secondary structure formed by agglomerating a plurality of primary particles. The average particle diameter of the secondary particles may be measured by using a particle size analyzer, and in the present invention, s3500 manufactured by Microtrac is used as a particle size analyzer.

[0040] Meanwhile, in the present invention, the proportion (%) of each crystallite or plurality of crystallites means (the number of the crystallites/the number of the total crystallites present in the region) $\times 100$.

[0041] Hereinafter, the present invention will be described in detail.

[0042] As a result of a significant amount of research conducted for developing a positive electrode active material capable of achieving excellent service life characteristics and resistance characteristics, the present inventors have found that when the crystallites having high long-axis orientation and low c-axis orientation are included in a particular proportion in the outer region of the positive electrode active material, capacity characteristics and gas generation characteristics of a secondary battery may be improved, thereby leading to the completion of the present invention.

Positive Electrode Active Material

[0043] A positive electrode active material according to the present invention, as shown in FIG. 1, is characterized by including an inner region 20 that is a region from the center of the positive electrode active material particle to R/2, and an outer region 10 that is a region from R/2 to the surface of the positive electrode active material particle, wherein R is the distance from the center of a positive electrode active material particle to the surface thereof. The proportion (C1) of the plurality of crystallites C is 25% to 80%, preferably 30% to 60%, more preferably 30% to 50%, and even more preferably 30% to 40% with respect to total crystallites in the outer region 10, wherein a crystallite long-axis orientation degree DoA represented by Equation 1 below is 0.5 to 1, and wherein a crystallite c-axis orientation degree represented by a cross product value of a c-axis rotation vector Rc of a crystal lattice of a crystallite obtained by electron backscatter diffraction (EBSD) analysis and a position unit vector P' of the crystallite is less than 0.5:

$$DoA = \frac{\lambda_1}{\lambda_1 + \lambda_2} C_D^2 \quad [\text{Equation 1}]$$

[0044] In Equation 1 above,

[0045] λ_1 is the size of a long-axis vector E_l of the crystallite determined from image data obtained by scanning ion microscope analysis of the cross-section of the positive electrode active material, λ_2 is the size of a short-axis vector E_{ll} of the crystallite determined from image data obtained by scanning ion microscope analysis of the cross-section of the positive electrode active material, and C_D above is an inner product value of a position unit vector P' and a long-axis vector E_l of the crystallite.

[0046] First, the DoA represented by Equation 1 above will be described.

[0047] The DoA value represented by Equation 1 above shows a long-axis orientation of the crystallites and can be determined by using data obtained through a scanning ion microscope analysis.

[0048] Specifically, a scanning ion microscope image may be obtained by irradiating the cross-section of the positive electrode active material with a focused ion beam, data segmented in a crystallite unit may be obtained from the scanning ion microscope image using deep learning, and a crystallite long-axis orientation degree DoA represented by Equation 1 above may be calculated from the segmented data.

[0049] Hereinafter, a method for calculating a DoA value through a scanning ion microscope analysis will be described in more detail.

[0050] A scanning ion microscope is a device for measuring the surface structure of a sample through the signal ion images generated when scanning the ion beam on the surface of the sample. In this case, since the ion beam has different reflectivity on different crystalline surfaces, the cross-sectional image of the positive electrode active material or a particle thereof distinguished in a unit of a single crystallite having the same atomic arrangement can be obtained using the scanning ion microscope. FIG. 1 shows a scanning ion microscope image of the cross-section of a positive electrode active material particle. Through FIG. 1, it can be confirmed that the cross-sectional image of the positive electrode active material particle is distinguished in a crystallite unit.

[0051] Next, the scanning ion microscope image thus obtained is analyzed to obtain data segmented in a crystallite unit. In this case, the image analysis may be performed using deep learning.

[0052] FIG. 2 shows a process of obtaining segmented data information by analyzing the scanning ion microscope image. As shown in FIG. 2, the image analysis may be performed by, for example, detecting a boundary from the scanning electron microscope image through deep learning and then obtaining image data segmented in a crystallite unit using the boundary.

[0053] In this case, the boundary detection may be performed using an AutoEncoder neural network (U-NET) algorithm, and the segmentation may be performed using a Watershed segmentation algorithm or the like.

[0054] Since the scanning ion microscope image itself does not include digitized information, in the present invention, data information segmented in each crystallite unit may be obtained through deep learning, and thus information such as the shape and position of the crystallites may be digitized.

[0055] When the segmented data are obtained through the scanning ion microscope image analysis, the position vector, long-axis vector, and short-axis vector of the crystallites to be determined may be calculated from the data, and using this, a DoA value in Equation 1 may be calculated.

$$DoA = \frac{\lambda_1}{\lambda_1 + \lambda_2} C_D^2 \quad [\text{Equation 1}]$$

[0056] In Equation 1 above,

[0057] λ_1 is the size of a long-axis vector E_l of the crystallite determined from image data obtained by the scanning ion microscope analysis of the cross-section of the

positive electrode active material, wherein the long-axis vector E_l means a vector having the smallest sum of distances between the vector and each pixel in the crystallite among vectors passing through the center of gravity of the crystallite.

[0058] λ_2 is the size of a short-axis vector E_{ll} of the crystallite determined from image data obtained by the scanning ion microscope analysis of the cross-section of the positive electrode active material, wherein the short-axis vector E_{ll} means a vector having the largest sum of distances between a single vector and each pixel in the crystallite among vectors passing through the center of gravity of the crystallite.

[0059] Meanwhile, C_D above is an inner product value of a position unit vector P' and the long-axis vector E_l' of the crystallite. The position unit vector P' of the crystallite is a vector obtained by converting the position vector, which connects from the center of the cross-section of the positive electrode active material particle to the center of gravity of the crystallite, into a size of 1. The long-axis unit vector E_l' is a vector obtained by converting the long-axis vector E_l into a size of 1.

[0060] The DoA value calculated by Equation 1 is a value showing how much the long-axis of the crystallite is inclined with respect to the shortest line passing through the crystallite and connecting the center of the positive electrode active material and the surface thereof, and means that the closer to 1 the DoA value, the smaller the angle between the long-axis of the crystallite and the shortest line, and the closer to 0 the DoA value, the larger the angle between the long-axis of the crystallite and the shortest line. That is, it can be said that the closer to 1 the DoA, the higher the long-axis orientation of the crystallite.

[0061] FIG. 3 shows a view in which the DoA value obtained by the method and the long-axis of the crystallite are indicated. As shown in FIG. 3, it can be seen that in the case of a crystallite 1 having a small angle between the crystallite long-axis and the shortest line connecting the center of the positive electrode active material particle and the surface thereof, the DoA is 0.965, which is close to 1, whereas in the case of a crystallite 2 having a large angle between the crystallite long-axis and the shortest line connecting the center of the positive electrode active material particle and the surface thereof, the DoA is 0.352, which is small.

[0062] Meanwhile, the proportion of the crystallites having a specific long-axis orientation value in the outer region and the proportion of such crystallites in the inner region of the positive electrode active material particle may be measured by mapping the long-axis orientation degree information of each crystallite as described above.

[0063] Next, the crystallite c-axis orientation degree will be described.

[0064] The crystallite c-axis orientation degree shows the orientation of a c-axis of a crystal lattice of a crystallite and is represented by a cross product value of a c-axis rotation vector R_c of the crystal lattice of the crystallite obtained by electron backscatter diffraction (EBSD) analysis and a position unit vector P' of the crystallite.

[0065] Specifically, the crystallite c-axis orientation degree may be determined by obtaining EBSD Euler map data including position information and Euler angle information on each crystallite through EBSD measurement of the cross-section of the positive electrode active material,

calculating the c-axis rotation vector Rc of the crystal lattice of the crystallite using the EBSD Euler map data, and calculating the cross product of the c-axis rotation vector Rc of the crystal lattice and the position unit vector P' of the crystallite.

[0066] Hereinafter, a method for determining the crystallite c-axis orientation degree according to the present invention will be described in detail.

[0067] The EBSD analysis is a method for measuring a crystallographic phase and a crystallographic orientation using a diffraction pattern of a sample and analyzing crystallographic information of the sample based on them. In the scanning electron microscope, if the sample (i.e., the cross-section of the positive electrode active material) is tilted to have a large angle with respect to the incident direction of the electron beam, the incident electron beam is scattered in the sample, and thus a diffraction pattern appears in the direction of the surface of the sample, which is called an Electron Back Scattered Diffraction Pattern (EBSP). Since the EBSP responds to the crystallographic orientation of the region irradiated with the electron beam, the crystallographic orientation of the sample may be accurately measured by using the EBSP, and Euler map data including various information related to the crystallographic orientation of the entire sample may be obtained through an EBSD software. FIG. 4 shows an Euler map obtained by performing the EBSD analysis on the cross-section of the positive electrode active material particle.

[0068] The EBSD Euler map data includes position vector information and Euler angle information of each crystallite. Meanwhile, by using the Euler angle information, the c-axis rotation vector Rc of the crystal lattice in each crystallite may be obtained.

[0069] The c-axis rotation vector Rc of the crystal lattice shows what direction the c-axis of the crystallite is rotated with respect to the shortest line passing through the crystallite and connecting the center of the positive electrode active material and the surface thereof.

[0070] Specifically, the c-axis rotation vector Rc of the crystal lattice may be (x, y, z) calculated by Equation 2 below:

$$\begin{bmatrix} x \\ y \\ z \end{bmatrix} = R_z(\Psi)R_y(\Theta)R_x(\Phi) \begin{bmatrix} X \\ Y \\ Z \end{bmatrix} = \begin{bmatrix} \cos\Psi & -\sin\Psi & 0 \\ \sin\Psi & \cos\Psi & 0 \\ 0 & 0 & 1 \end{bmatrix} \begin{bmatrix} \cos\Theta & 0 & \sin\Theta \\ 0 & 1 & 0 \\ -\sin\Theta & 0 & \cos\Theta \end{bmatrix} \begin{bmatrix} 1 & 0 & 0 \\ 0 & \cos\Phi & -\sin\Phi \\ 0 & \sin\Phi & \cos\Phi \end{bmatrix} \begin{bmatrix} X \\ Y \\ Z \end{bmatrix} = \begin{bmatrix} \cos\Theta\cos\Psi & -\cos\Theta\sin\Psi + \sin\Phi\sin\Theta\cos\Psi & \sin\Phi\sin\Psi + \cos\Phi\sin\Theta\cos\Psi \\ \cos\Theta\sin\Psi & \cos\Phi\cos\Psi + \sin\Phi\sin\Theta\sin\Psi & -\sin\Phi\cos\Psi + \cos\Phi\sin\Theta\sin\Psi \\ -\sin\Theta & \sin\Phi\cos\Theta & \cos\Phi\cos\Theta \end{bmatrix} \begin{bmatrix} X \\ Y \\ Z \end{bmatrix}$$

[0071] In Equation 2 above, [X, Y, Z] is (0, 0, 1), and Φ , θ , and Ψ above each represent an Euler angle of each crystallite obtained from the Euler map data.

[0072] A crystallite c-axis orientation degree may be obtained by using the c-axis rotation vector Rc of the crystal lattice as obtained above and the position vector information of each crystallite included in the Euler map data. Specifically, the crystallite c-axis orientation degree may be digitized as a value obtained by calculating a cross product of

the c-axis rotation vector Rc of the crystal lattice and the position unit vector P' of the crystallite.

[0073] In this case, the position unit vector P' means that the position vector of the crystallite is converted to have a size of 1. For example, if the position vector of the crystallite is (a, b, 0), the position unit vector becomes

$$\left(\frac{a}{\sqrt{a^2 + b^2}}, \frac{b}{\sqrt{a^2 + b^2}}, 0 \right).$$

[0074] A cross product value of the position unit vector P' and the c-axis rotation vector Rc of the crystal lattice is a numerical value showing the c-axis orientation degree of the crystallite in the positive electrode active material particle. Specifically, in the case where the cross product value of the position unit vector P' and the c-axis rotation vector Rc of the crystal lattice is 1, the c-axis of the crystallite is disposed perpendicular to the shortest line connecting the center of the positive electrode active material particle and the surface thereof. In the case where the cross product value is 0, the c-axis of the crystallite is disposed parallel to the shortest line.

[0075] In the positive electrode active material, the mobility of lithium ions when moving along the direction perpendicular to the c-axis is at least 10 times faster than when moving in the c-axis direction. Accordingly, a lithium path is formed along the direction perpendicular to the c-axis. In addition, when the lithium path is formed parallel to the shortest line connecting the center of the positive electrode active material particle and the surface thereof, a lithium moving distance is minimized, and thus lithium conductivity is improved. Therefore, it may be determined that the c-axis orientation of the crystallite is excellent as the cross product value of the position unit vector P' and the c-axis rotation vector Rc of the crystal lattice is closer to 1.

[0076] Meanwhile, by collecting the c-axis orientation degree of each crystallite as obtained above, the c-axis orientation degree of the total crystallites in the cross-section of the positive electrode active material particle may be

[Equation 2]

obtained. FIG. 5 shows a crystallite c-axis orientation map of the positive electrode active material obtained by collecting the c-axis orientation degree of each crystallite. In FIG. 5, the c-axis orientation becomes superior as it goes closer to red, and the c-axis orientation becomes inferior as it goes closer to blue. By using the c-axis orientation map as described above, the proportions of the crystallites satisfying the c-axis orientation condition in the outer region and the inner region of the positive electrode active material particle may be obtained.

[0077] According to the study of the present inventors, it has been found that when the proportion (hereinafter, referred to as C1) of the plurality of crystallites (hereinafter, referred to as crystallites C) satisfies 25% to 80%, and preferably 30% to 60% with respect to the total crystallites in the outer region of the positive electrode active material, wherein a crystallite long-axis orientation degree DoA represented by Equation 1 is 0.5 to 1 and a crystallite c-axis orientation degree is less than 0.5, excellent capacity characteristics and gas generation characteristics may be achieved. When the proportion of the crystallites C in the outer region is less than 25% or greater than 80%, an effect of improving capacity characteristics and gas generation characteristics is slight.

[0078] In addition, the positive electrode active material of the present invention may have the proportion (C1) of the crystallites C in the outer region larger than the proportion (C2) of the crystallites C in the inner region. When the proportion of the crystallites C in the outer region is larger than in the inner region, a more excellent effect of suppressing the gas generation is exhibited.

[0079] Specifically, the difference between the proportion (C1) of the crystallites C to the total crystallites in the outer region and the proportion (C2) of the crystallites C to the total crystallites in the inner region may be at least 3%, at least 5%, 3% to 20%, or 3% to 15%. When the difference between the proportions of the crystallites C in the outer region and the inner region satisfies the above range, an effect of improving the capacity and an effect of reducing the gas generation is excellent. If the difference between the proportions of the crystallites C in the outer region and the inner region is high, further improved effect may be obtained.

[0080] Meanwhile, in addition to the crystallites C, the positive electrode active material according to the present invention may further include, in the outer region, the inner region, or both, crystallites having a crystallite c-axis orientation degree of 0.5 to 1 and a crystallite long-axis orientation degree DoA of 0.5 to 1 (hereinafter, referred to as crystallites A), crystallites having a crystallite c-axis orientation degree of 0.5 to 1 and a crystallite long-axis orientation degree DoA of less than 0.5 (hereinafter, referred to as crystallites B), and crystallites having a crystallite c-axis orientation degree of less than 0.5 and a crystallite long-axis orientation degree DoA of less than 0.5 (hereinafter, referred to as crystallites D).

[0081] Meanwhile, in the positive electrode active material of the present invention, the proportion (C1) of the crystallites C to the total grains or total crystallites in the outer region may be larger than each proportion of other crystallites, that is, the proportion (A1) of the crystallites A, the proportion (B1) of the crystallites B, and the proportion (D1) of the crystallites D. That is, $C1 > B1$, $C1 > A1$, and $C1 > D1$ are preferably satisfied.

[0082] The larger the contact area of a movement path of lithium ions (Li path) and an electrolyte solution during charge and discharge, the more the gas is generated and the more rapidly the deterioration of the structure occurs. In the case of the crystallites C having low c-axis orientation degree, the contact area of the electrolyte solution and the plane direction of the ab-plane which is a lithium movement path inside the crystallites is small, and thus an amount of gas generated is small. On the contrary, in the case of the crystallites A and crystallites B, since the c-axis orientation

degree is large, the contact area of the electrolyte solution and the plane direction of the ab-plane is large, and thus when the crystallites A or crystallites B are present in the outer region in a high proportion, an amount of gas generated is increased.

[0083] Meanwhile, in the case of the crystallites D, an amount of gas generated is small, but since both the c-axis orientation degree and the long-axis orientation degree are low, intercalation and deintercalation of lithium ions are difficult, and thus capacity characteristics are significantly decreased. On the contrary, in the case of the crystallites C, due to high long-axis orientation degree, the movement distance of lithium ions which move along the interface between the crystallite and the crystallite during charge and discharge is short, and thus excellent capacity characteristics may be achieved.

[0084] Thus, if the proportion (C1) of the crystallites C to the total crystallites in the outer region is higher than each proportion of the other crystallites, excellent gas generation characteristics and capacity characteristics may both be achieved.

[0085] Meanwhile, in the positive electrode active material according to the present invention, the proportion of the crystallites A to the total crystallites in the cross-section of the positive electrode active material particle may be 5% to 40%, preferably, 10% to 30%, the proportion of the crystallites B may be 5% to 40%, preferably, 10% to 30%, the proportion of the crystallites C may be 20% to 80%, preferably, 25% to 60%, and the proportion of the crystallites D may be 5% to 40%, preferably, 10% to 30%. When the proportion of the crystallites in the whole positive electrode active material satisfies the above range, the effect of suppressing the gas generation and the effect of improving the capacity are more excellent.

[0086] Meanwhile, since the proportion of the crystallites of the positive electrode active material varies depending on the composition of a precursor used in the preparation of the positive electrode active material, the shape and orientation of the crystallite of the precursor, the type of doping elements, and/or firing temperature, etc., the positive electrode active material satisfying the proportion of the crystallites of the present invention may be prepared by appropriately adjusting the type of precursors, the doping elements, the firing temperature, etc.

[0087] Meanwhile, the positive electrode active material according to the present invention may be a lithium composite transition metal oxide including two or more transition metals, for example, it may be a lithium composite transition metal oxide represented by Formula 1 below:



[0088] In Formula 1, M^1 above may be at least one element selected from the group consisting of Mn and Al.

[0089] M^2 above may be at least one element selected from the group consisting of W, Cu, Fe, V, Cr, Ti, Zr, Zn, Al, Ta, Y, In, La, Sr, Ga, Sc, Gd, Sm, Ca, Ce, Nb, Mg, B, and Mo.

[0090] In addition, A above may be at least one element selected from the group consisting of F, Cl, Br, I, At, and S.

[0091] x above represents a ratio of the moles of Li to the total moles of transition metals, wherein x may satisfy $0.98 \leq x \leq 1.20$, preferably $0.99 \leq x \leq 1.10$, and more preferably 1.0×1.10 .

[0092] a above represents a ratio of the moles of Ni to the total moles of transition metals, wherein a may satisfy $0 < a < 1$, preferably $0.3 \leq a < 1$, more preferably $0.6 \leq a < 1$, even more preferably $0.8 \leq a < 1$, and still even more preferably $0.85 \leq a < 1$.

[0093] b above represents a ratio of the moles of Co to the total moles of transition metals, wherein b may satisfy $0 < b < 1$, preferably $0 < b < 0.7$, more preferably $0 < b < 0.4$, even more preferably $0 < b < 0.2$, and still even more preferably $0 \leq b \leq 0.1$.

[0094] c above represents a ratio of the moles of M^1 to the total moles of transition metals, wherein c may satisfy $0 < c < 1$, preferably $0 < c < 0.7$, more preferably $0 < c < 0.4$, even more preferably $0 < c < 0.2$, and still even more preferably $0 < c \leq 0.1$.

[0095] d above represents a ratio of the moles of M^2 to the total moles of transition metals, wherein d may satisfy $0 \leq d \leq 0.2$, preferably $0 \leq d \leq 0.15$, and more preferably $0 \leq d \leq 0.10$.

[0096] y above represents a ratio of the moles of element A substituted at the position of oxygen, wherein y may satisfy $0 \leq y \leq 0.2$, preferably $0 \leq y \leq 0.15$, and more preferably $0 \leq y \leq 0.10$.

[0097] Meanwhile, the positive electrode active material may have a crystallite size of 100 nm to 200 nm, preferably 100 nm to 180 nm, and more preferably 100 nm to 150 nm. If the size of the crystallite becomes too large, a rock salt phase may be formed, and thus resistance characteristics and service life characteristics may be degraded, and if the size of the crystallite becomes too small, a contact area with an electrolyte solution may increase, and thus the deterioration may occur rapidly.

[0098] In addition, the positive electrode active material may have an average particle diameter of primary particles of 0.05 μm to 4 μm , and preferably 0.1 μm to 2 μm . If the average particle diameter of the primary particles is too large, a rock salt phase may be formed, and thus resistance characteristics and service life characteristics may be degraded, and if the average particle diameter of the primary particles is too small, a contact area with an electrolyte solution may increase, and thus the deterioration may occur rapidly.

[0099] In addition, the positive electrode active material may have an average particle diameter of secondary particles of 2 μm to 25 μm , and preferably 4 μm to 18 μm . When the average particle diameter of the secondary particles satisfies the above range, it is possible to prevent the cathode active material particles from being broken in the rolling process or the processability from deteriorating during the preparation of the slurry.

Positive Electrode

[0100] Next, a positive electrode according to the present invention will be described.

[0101] The positive electrode includes the positive electrode active material according to the present invention. Specifically, the positive electrode includes a positive electrode current collector and a positive electrode active material layer formed on the positive electrode current collector, wherein the positive electrode active material layer includes the positive electrode active material according to the present invention.

[0102] In this case, since the positive electrode active material is the same as described above, detailed descrip-

tions thereof will be omitted, and the remaining configurations will be only described in detail below.

[0103] The positive electrode current collector may include a metal having high conductivity, and is not particularly limited as long as the positive electrode active material layer easily adheres thereto and there is no reactivity in the voltage range of the battery. For example, stainless steel, aluminum, nickel, titanium, fired carbon, or aluminum or stainless steel that is surface-treated with one of carbon, nickel, titanium, silver, or the like may be used as or in the positive electrode current collector. Also, the positive electrode current collector may typically have a thickness of 3 μm to 500 μm , and microscopic irregularities may be formed on the surface of the current collector to improve the adhesion of the positive electrode active material. For example, the positive electrode current collector may be used in various forms such as a film, a sheet, a foil, a net, a porous body, a foam, and a non-woven body.

[0104] The positive electrode active material layer may optionally include a conductive agent, a binder, etc., if necessary, in conjunction with the positive electrode active material.

[0105] In this case, the positive electrode active material may be included in an amount of 80 wt % to 99 wt %, for example, 85 wt % to 98.5 wt % based on a total weight of the positive electrode active material layer. When the positive electrode active material is included in an amount within the above range, excellent capacity characteristics may be obtained.

[0106] The conductive agent is used to provide conductivity to the electrode, wherein any conductive agent may be used without particular limitation as long as it has suitable electron conductivity without causing adverse chemical changes in the battery. Specific examples of the conductive agent may be graphite such as natural graphite or artificial graphite; carbon based materials such as carbon black, acetylene black, Ketjen black, channel black, furnace black, lamp black, thermal black, and carbon fibers; powder or fibers of metals such as copper, nickel, aluminum, and silver; conductive tubes such as carbon nanotubes; conductive whiskers such as zinc oxide whiskers and potassium titanate whiskers; conductive metal oxides such as titanium oxide; or conductive polymers such as polyphenylene derivatives, and any one thereof or a mixture of two or more thereof may be used. The conductive agent may be included in an amount of 0.1 wt % to 15 wt % based on the total weight of the positive electrode active material layer.

[0107] The binder improves the adhesion between the positive electrode active material particles and the adhesion between the positive electrode active material and the current collector. Specific examples of the binder may be polyvinylidene fluoride (PVDF), polyvinylidene fluoride-hexafluoropropylene copolymer (PVDF-co-HFP), polyvinyl alcohol, polyacrylonitrile, polymethylmethacrylate, carboxymethyl cellulose (CMC), starch, hydroxypropyl cellulose, regenerated cellulose, polyvinylpyrrolidone, polytetrafluoroethylene, polyethylene, polypropylene, an ethylene-propylene-diene monomer (EPDM), a sulfonated EPDM, a styrene-butadiene rubber (SBR), a fluorine rubber, polyacrylic acid, and a polymer having hydrogen thereof substituted with Li, Na, or Ca, or various copolymers thereof, and any one thereof or a mixture of two or more thereof may be used. The binder may be included in an amount of 0.1 wt

% to 15 wt % based on the total weight of the positive electrode active material layer.

[0108] The positive electrode may be prepared according to a typical method of preparing a positive electrode except that the above-described positive electrode active material is used. Specifically, a positive electrode slurry composition, which is prepared by dissolving or dispersing optionally the binder, the conductive agent, and the dispersing agent, if necessary, as well as the positive electrode active material in a solvent, is coated on the positive electrode collector, and the positive electrode may then be prepared by drying and rolling the coated positive electrode current collector.

[0109] The solvent may be a solvent normally used in the art. The solvent may include dimethyl sulfoxide (DMSO), isopropyl alcohol, N-methylpyrrolidone (NMP), dimethyl formamide (DMF), acetone, or water, and any one thereof or a mixture of two or more thereof may be used. An amount of the solvent used may be sufficient if the solvent may dissolve or disperse the positive electrode active material, the conductive agent, the binder, and the dispersing agent in consideration of a coating thickness of the slurry and manufacturing yield, and may have a viscosity that provides excellent thickness uniformity during the subsequent coating for the preparation of the positive electrode.

[0110] Also, as another method, the positive electrode may be prepared by casting the positive electrode slurry composition on a separate support and then laminating a film separated from the support on the positive electrode collector.

Secondary Battery

[0111] Furthermore, in the present invention, an electrochemical device including the positive electrode may be prepared. The electrochemical device may specifically be a battery or a capacitor, and, for example, may be a lithium secondary battery.

[0112] The lithium secondary battery may specifically include a positive electrode, a negative electrode disposed to face the positive electrode, a separator disposed between the positive electrode and the negative electrode, and an electrolyte. Since the positive electrode is the same as described above, detailed descriptions thereof will be omitted, and the remaining configurations will be only described in detail below.

[0113] Also, the lithium secondary battery may further optionally include a battery container accommodating an electrode assembly of the positive electrode, the negative electrode, and the separator, and a sealing member for sealing the battery container.

[0114] In the lithium secondary battery, the negative electrode includes a negative electrode current collector and a negative electrode active material layer disposed on the negative electrode current collector.

[0115] The negative electrode current collector is not particularly limited as long as it has high conductivity without causing adverse chemical changes in the battery, and, for example, copper, stainless steel, aluminum, nickel, titanium, fired carbon, copper or stainless steel that is surface-treated with one of carbon, nickel, titanium, silver, or the like, and an aluminum-cadmium alloy may be used. Also, the negative electrode collector may typically have a thickness of 3 μm to 500 μm , and as in the case of the positive electrode current collector, microscopic irregularities may be formed on the surface of the negative electrode

current collector to improve the adhesion of a negative electrode active material. For example, the negative electrode current collector may be used in various forms such as a film, a sheet, a foil, a net, a porous body, a foam, and a non-woven body.

[0116] The negative electrode active material layer optionally includes a binder and a conductive agent in addition to the negative electrode active material.

[0117] A compound capable of reversibly intercalating and deintercalating lithium may be used as the negative electrode active material. Specific examples of the negative electrode active material may be a carbonaceous material such as artificial graphite, natural graphite, graphitized carbon fibers, and amorphous carbon; a metallic compound alloyable with lithium such as Si, Al, Sn, Pb, Zn, Bi, In, Mg, Ga, Cd, a Si alloy, a Sn alloy, or an Al alloy; a metal oxide which may be doped and undoped with lithium such as SiO_β ($0 < \beta < 2$), SnO_2 , vanadium oxide, and lithium vanadium oxide; or a composite including the metallic compound and the carbonaceous material such as a Si—C composite or a Sn—C composite, and any one thereof or a mixture of two or more thereof may be used. Also, a metallic lithium thin film may be used as the negative electrode active material. Furthermore, both low crystalline carbon and high crystalline carbon may be used as the carbon material. Typical examples of the low crystalline carbon may be soft carbon and hard carbon, and typical examples of the high crystalline carbon may be irregular, planar, flaky, spherical, or fibrous natural graphite or artificial graphite, Kish graphite, pyrolytic carbon, mesophase pitch-based carbon fibers, meso-carbon microbeads, mesophase pitches, and high-temperature fired carbon such as petroleum or coal tar pitch derived cokes.

[0118] The negative electrode active material may be included in an amount of 80 wt % to 99 wt % based on a total weight of the negative electrode active material layer.

[0119] The binder is a component that assists in the binding between the conductive agent, the active material, and the current collector, wherein the binder is commonly added in an amount of 0.1 wt % to 10 wt % based on the total weight of the negative electrode active material layer. Examples of the binder may include a polyvinylidene fluoride (PVDF), a polyvinyl alcohol, carboxymethylcellulose (CMC), starch, hydroxypropyl cellulose, regenerated cellulose, polyvinylpyrrolidone, polytetrafluoroethylene, polyethylene, polypropylene, an ethylene-propylene-diene polymer (EPDM), a sulfonated EPDM, a styrene-butadiene rubber, a nitrile-butadiene rubber, a fluoro rubber, various copolymers thereof, and the like.

[0120] The conductive agent is a component for further improving conductivity of the negative electrode active material, wherein the conductive agent may be added in an amount of 10 wt % or less, for example, 5 wt % or less based on the total weight of the negative electrode active material layer. The conductive agent is not particularly limited as long as it has conductivity without causing adverse chemical changes in the battery. For example, graphite such as natural graphite or artificial graphite; carbon black such as acetylene black, Ketjen black, channel black, furnace black, lamp black, and thermal black; conductive fibers such as carbon fibers or metal fibers; fluorocarbons; metal powder such as aluminum powder or nickel powder; a conductive whisker such as a zinc oxide whisker or a potassium titanate whisker;

a conductive metal oxide such as a titanium oxide; or a conductive material such as a polyphenylene derivative; and the like may be used.

[0121] The negative electrode active material layer may be prepared, for example, by coating a negative electrode slurry composition, which is prepared by dissolving or dispersing optionally the binder and the conductive agent as well as the negative electrode active material in a solvent, on the negative electrode current collector and drying the coated negative electrode current collector, or may be prepared by casting the negative electrode slurry composition on a separate support and then laminating a film separated from the support on the negative electrode current collector.

[0122] In the lithium secondary battery, the separator separates the negative electrode and the positive electrode and provides a movement path of lithium ions, wherein any separator may be used as the separator without particular limitation as long as it is typically used in a lithium secondary battery, and particularly, a separator having high moisture-retention ability for an electrolyte solution as well as low resistance to the transfer of electrolyte ions may be used. Specifically, a porous polymer film, for example, a porous polymer film prepared from a polyolefin-based polymer, such as an ethylene homopolymer, a propylene homopolymer, an ethylene/butene copolymer, an ethylene/hexene copolymer, and an ethylene/methacrylate copolymer, or a laminated structure having two or more layers thereof may be used. Also, a typical porous nonwoven fabric, for example, a nonwoven fabric formed of high melting point glass fibers or polyethylene terephthalate fibers may be used. Furthermore, a coated separator including a ceramic component or a polymer material may be used to secure heat resistance or mechanical strength, and may be optionally used in a single-layered or multi-layered structure.

[0123] In addition, an electrolyte used in the present invention may include an organic liquid electrolyte, an inorganic liquid electrolyte, a solid polymer electrolyte, a gel-type polymer electrolyte, a solid inorganic electrolyte, or a molten-type inorganic electrolyte which may be used in the manufacture of the lithium secondary battery, but is not limited thereto.

[0124] Specifically, the electrolyte may include an organic solvent and a lithium salt.

[0125] Any organic solvent may be used as the organic solvent without particular limitation so long as it may function as a medium through which ions involved in an electrochemical reaction of the battery may move. Specifically, an ester-based solvent such as methyl acetate, ethyl acetate, γ -butyrolactone, and ϵ -caprolactone; an ether-based solvent such as dibutyl ether or tetrahydrofuran; a ketone-based solvent such as cyclohexanone; an aromatic hydrocarbon-based solvent such as benzene and fluorobenzene; or a carbonate-based solvent such as dimethyl carbonate (DMC), diethyl carbonate (DEC), methylethyl carbonate (MEC), ethylmethyl carbonate (EMC), ethylene carbonate (EC), and propylene carbonate (PC); an alcohol-based solvent such as ethyl alcohol and isopropyl alcohol; nitriles such as R—CN (where R is a linear, branched, or cyclic C2-C20 hydrocarbon group and may include a double-bond aromatic ring or ether bond); amides such as dimethylformamide; dioxolanes such as 1,3-dioxolane; or sulfolanes may be used as the organic solvent. Among these solvents, the carbonate-based solvent may be used, and, for example,

a mixture of a cyclic carbonate (e.g., ethylene carbonate or propylene carbonate) having high ionic conductivity and high dielectric constant, which may increase charge/discharge performance of the battery, and a low-viscosity linear carbonate-based compound (e.g., ethylmethyl carbonate, dimethyl carbonate, or diethyl carbonate) may be used.

[0126] The lithium salt may be used without particular limitation as long as it is a compound capable of providing lithium ions used in the lithium secondary battery. Specifically, anions of the lithium salt may be at least one selected from the group consisting of F^- , Cl^- , Br^- , I^- , NO_3^- , $N(CN)_2^-$, BF_4^- , $CF_3CF_2SO_3^-$, $(CF_3SO_2)_2N^-$, $(FSO_2)_2N^-$, $CF_3CF_2(CF_3)_2CO^-$, $(CF_3SO_2)_2CH^-$, $(SF_5)_3C^-$, $(CF_3SO_2)_3C^-$, $CF_3(CF_2)_7SO_3^-$, $CF_3CO_2^-$, $CH_3CO_2^-$, SCN^- , and $(CF_3CF_2SO_2)_2N^-$, and as the lithium salt, $LiPF_6$, $LiClO_4$, $LiAsF_6$, $LiBF_4$, $LiSbF_6$, $LiAlO_4$, $LiAlCl_4$, $LiCF_3SO_3$, $LiC_4F_9SO_3$, $LiN(C_2F_5SO_3)_2$, $LiN(C_2F_5SO_2)_2$, $LiN(CF_3SO_2)_2$, $LiCl$, LiI , $LiB(C_2O_4)_2$, or the like may be used. It is preferable to use the lithium salt in a concentration range of 0.1 M to 2.0 M. When the concentration of the lithium salt is in the above range, the electrolyte may have suitable conductivity and viscosity, thereby exhibiting excellent performance, and lithium ions may effectively move.

[0127] The lithium secondary battery including the positive electrode active material according to the present invention as describe above exhibits excellent capacity characteristics and service life characteristics, and may be useful for various fields such as portable devices such as a mobile phone, a notebook computer, and a digital camera, or electric cars.

[0128] Hereinafter, the present invention will be described in detail, according to specific examples. The invention may, however, be embodied in many different forms and should not be construed as being limited to the embodiments set forth herein. Rather, these example embodiments are provided so that this description will be thorough and complete, and will fully convey the scope of the present invention to those skilled in the art.

EXAMPLES

Preparation Example 1—Preparation of Positive Electrode Active Material Precursor A

[0129] $NiSO_4$, $CoSO_4$, and $MnSO_4$ were mixed in distilled water in an amount such that a molar ratio of nickel:cobalt:manganese was 92:4:4 to prepare a 2.4 M transition metal aqueous solution.

[0130] Then, after deionized water was put into a reactor, dissolved oxygen in the water was removed by purging the reactor with nitrogen gas to create a non-oxidizing atmosphere in the reactor. Thereafter, 7.96 M NaOH was added thereto so that a pH in the reactor was maintained at 11.9.

[0131] Thereafter, while the transition metal aqueous solution, a NaOH aqueous solution, and a NH_4OH aqueous solution were added to the reactor at rates of 850 mL/hr, 510 mL/hr, and 160 mL/hr, respectively, a co-precipitation reaction was performed for 40 hours at a reaction temperature of 50° C., a pH of 11.4, and a stirring speed of 600 rpm to prepare a positive electrode active material precursor A which had an average particle diameter (D_{50}) of 15 μm and was represented by $Ni_{0.92}Co_{0.04}Mn_{0.04}(OH)_2$.

Preparation Example 2—Preparation of Positive
Electrode Active Material Precursor B

[0132] A positive electrode active material precursor B which has an average particle diameter (D_{50}) of 4 μm and is represented by $\text{Ni}_{0.92}\text{Co}_{0.04}\text{Mn}_{0.04}(\text{OH})_2$ was prepared in the same manner as in Preparation Example 1 except that the co-precipitation reaction was performed for 12 hours.

Example 1

[0133] The positive electrode active material precursor A prepared in Preparation Example 1 and LiOH were mixed in an amount such that a molar ratio of Li:transition metals (Ni+Co+Mn) was 1.05:1, Nb_2O_3 was added thereto and mixed such that a molar ratio of transition metals (Ni+Co+Mn):Nb was 99.75:0.25, and the resultant mixture was fired at 770° C. for 13 hours to prepare $\text{Li}[\text{Ni}_{0.92}\text{Co}_{0.04}\text{Mn}_{0.04}]_{0.9975}\text{Nb}_{0.0025}\text{O}_2$.

[0134] Then, the $\text{Li}[\text{Ni}_{0.92}\text{Co}_{0.04}\text{Mn}_{0.04}]_{0.9975}\text{Nb}_{0.0025}\text{O}_2$ was washed with water and dried, then mixed with 500 ppm of boric acid, and heat-treated at 300° C. to prepare a positive electrode active material coated with B.

Example 2

[0135] A positive electrode active material was prepared in the same manner as in Example 1 except that the firing was performed at 790° C.

Example 3

[0136] The positive electrode active material precursor A prepared in Preparation Example 1 and LiOH were mixed in an amount such that a molar ratio of Li:transition metals

(Ni+Co+Mn) was 1.05:1, MgO was added thereto and mixed such that a molar ratio of transition metals (Ni+Co+Mn):Mg was 99.75:0.25, and the resultant mixture was fired at 770° C. for 13 hours to prepare $\text{Li}[\text{Ni}_{0.92}\text{Co}_{0.04}\text{Mn}_{0.04}]_{0.9975}\text{Mg}_{0.0025}\text{O}_2$.

[0137] Then, the $\text{Li}[\text{Ni}_{0.92}\text{Co}_{0.04}\text{Mn}_{0.04}]_{0.9975}\text{Mg}_{0.0025}\text{O}_2$ was washed with water and dried, then mixed with 500 ppm of boric acid, and heat-treated at 300° C. to prepare a positive electrode active material coated with B.

Comparative Example 1

[0138] The positive electrode active material precursor A prepared in Preparation Example 1 and LiOH were mixed in

an amount such that a molar ratio of Li:transition metals (Ni+Co+Mn) was 1.05:1, and the resultant mixture was fired at 780° C. for 13 hours to prepare $\text{Li}[\text{Ni}_{0.92}\text{Co}_{0.04}\text{Mn}_{0.04}]\text{O}_2$.

[0139] Then, the $\text{Li}[\text{Ni}_{0.92}\text{Co}_{0.04}\text{Mn}_{0.04}]\text{O}_2$ was washed with water and dried, then mixed with 500 ppm of boric acid, and heat-treated at 300° C. to prepare a positive electrode active material coated with B.

Comparative Example 2

[0140] The positive electrode active material precursor B prepared in Preparation Example 2 and LiOH were mixed in an amount such that a molar ratio of Li:transition metals (Ni+Co+Mn) was 1.07:1, Nb_2O_3 was added thereto and mixed such that a molar ratio of transition metals (Ni+Co+Mn):Nb was 99.75:0.25, and the resultant mixture was fired at 770° C. for 13 hours to prepare $\text{Li}[\text{Ni}_{0.92}\text{Co}_{0.04}\text{Mn}_{0.04}]_{0.9975}\text{Nb}_{0.0025}\text{O}_2$.

[0141] Then, the $\text{Li}[\text{Ni}_{0.92}\text{Co}_{0.04}\text{Mn}_{0.04}]_{0.9975}\text{Nb}_{0.0025}\text{O}_2$ was washed with water and dried, then mixed with 500 ppm of boric acid, and heat-treated at 300° C. to prepare a positive electrode active material coated with B.

Experimental Example 1

[0142] Each of the positive electrode active materials prepared according to Examples 1 to 3 and Comparative Examples 1 and 2 was cut by using an ion milling system (Hitachi, IM4000), and then the proportion of crystallites A, B, C, and D in the outer region and the inner region was measured by performing the scanning electron ion microscope analysis and EBSD analysis.

[0143] Measurement results are shown in Table 1 below:

TABLE 1

	Proportion (%) of crystallites in outer region				Proportion (%) of crystallites in inner region				Proportion of crystallites C in outer region – proportion of crystallites C in inner region
	A	B	C	D	A	B	C	D	
Example 1	21	23.6	34.5	20.9	21.3	25.3	26.4	27	8.1
Example 2	22.1	23	33.4	33.4	21.5	22.8	29.7	16.5	3.7
Example 3	27.5	23.6	32.1	16.8	20	27	27.1	25.9	5
Comparative Example 1	20.9	28.3	24.6	26.2	21.9	23.3	26.0	28.8	-1.4
Comparative Example 2	8.9	3.6	80.4	7.1	14.3	9.5	71.4	4.8	9

Experimental Example 2: Evaluation of Battery Characteristics

[0144] Each of the positive electrode active materials prepared in Examples 1 to 3 and Comparative Examples 1 and 2, a conductive agent (Denka black), and a binder (PVDF) were mixed in an N-methyl-2-pyrrolidone (NMP) solvent in a weight ratio of 97.5:1:1.5 to prepare a positive electrode slurry. One surface of an aluminum current collector was coated with the positive electrode slurry, dried, and then rolled to prepare a positive electrode.

[0145] A lithium metal electrode was used as a negative electrode.

[0146] Each lithium secondary battery was prepared by preparing an electrode assembly by disposing a separator between the positive electrode and the negative electrode, disposing the electrode assembly in a battery case, and then injecting an electrolyte solution. In this case, an electrolyte solution was used in which 1 M LiPF₆ was dissolved in an organic solvent in which ethylene carbonate, ethylmethyl carbonate, and diethyl carbonate were mixed in a volume ratio of 3:3:4.

[0147] Then, each of the secondary batteries was charged to 4.2V at a constant current of 0.1 C at 25° C. Thereafter, each of the secondary batteries was discharged to 3 V at a constant current of 0.1 C to measure initial charge capacity and initial discharge capacity. Measurement results are shown in Table 2 below.

[0148] In addition, each of positive electrode active materials prepared in Examples 1 to 3 and Comparative Examples 1 and 2, a conductive agent (Denka black), and a binder (PVDF) were mixed in an N-methyl-2-pyrrolidone (NMP) solvent in a weight ratio of 97.5:1.0:1.5 to prepare a positive electrode slurry. One surface of an aluminum current collector was coated with the positive electrode slurry, dried, and then rolled to prepare a positive electrode.

[0149] Next, a negative electrode active material (natural graphite), a conductive agent (carbon black), and a binder (PVDF) were mixed in an N-methylpyrrolidone solvent in a weight ratio of 95.6:1.0:3.4 to prepare a negative electrode slurry. A copper current collector was coated with the negative electrode slurry composition, dried, and then rolled to prepare a negative electrode.

[0150] Each lithium secondary battery was prepared by preparing an electrode assembly by disposing a separator between the positive electrode and the negative electrode, disposing the electrode assembly in a battery case, and then injecting an electrolyte solution. In this case, an electrolyte solution was used in which 0.7 M LiPF₆ was dissolved in an organic solvent in which ethylene carbonate and ethylmethyl carbonate were mixed in a volume ratio of 3:7.

[0151] Then, each of the lithium secondary batteries was charged to 4.2 V at a constant current of 0.1 C at 25° C. Thereafter, each of the lithium secondary batteries was discharged to 3 V at a constant current of 0.1 C (one cycle), and then 200 cycles of charge and discharge were performed in a range of 3 V to 4.2 V at 0.33 C at 45° C.

[0152] The lithium secondary battery charged and discharged for one cycle and the lithium secondary battery charged and discharged for 200 cycles were each perforated in a vacuum atmosphere chamber, and the gas inside the battery was emitted and captured inside the vacuum chamber. The gas in the chamber was quantitatively analyzed with a gas chromatograph-flame ionization detector (GC-FID) to measure a gas generation amount. Then, the gas generation amount in the lithium secondary battery charged and discharged for 200 cycles was divided by the gas generation amount in the lithium secondary battery charged and discharged for one cycle, and then multiplied by 100 to calculate a gas increase rate (%)

TABLE 2

	Charge capacity (mAh/g)	Discharge capacity (mAh/g)	Gas increase rate (%)
Example 1	244.8	227.7	130
Example 2	239.2	220.5	151

TABLE 2-continued

	Charge capacity (mAh/g)	Discharge capacity (mAh/g)	Gas increase rate (%)
Example 3	242.5	222.4	149
Comparative Example 1	226.5	204.8	252
Comparative Example 2	240.5	213.2	312

[0153] As shown in Table 2 above, the secondary batteries using the positive electrode active materials of Examples 1 to 3, in which the proportion of the crystallites C in the outer region of the positive electrode active material particle satisfies the range of the present invention, had more excellent capacity characteristics and generated less gas as compared with the secondary batteries using the positive electrode active materials of Comparative Examples 1 and 2. In addition, for the positive electrode active materials of Example 1 and Example 3, in which the difference between the proportions of crystallites C in the outer region and the inner region is large by at least 5%, such an improvement effect was more excellent.

1. A positive electrode active material comprising:
 - an inner region that is a region from a center of a positive electrode active material particle to R/2; and
 - an outer region that is a region from R/2 to a surface of the positive electrode active material particle,
 wherein R is a distance from the center of the positive electrode active material particle to the surface thereof, wherein a proportion (C1) of a plurality of crystallites C is 25% to 80% with respect to a total number of crystallites in the outer region, wherein a crystallite long-axis orientation degree DoA represented by Equation 1 below is 0.5 to 1, and wherein a crystallite c-axis orientation degree represented by a cross product value of a c-axis rotation vector Rc of a crystal lattice of a crystallite obtained by electron backscatter diffraction (EBSD) analysis and a position unit vector P' of the crystallite is less than 0.5:

$$DoA = \frac{\lambda_1}{\lambda_1 + \lambda_2} C_D^2 \quad [\text{Equation 1}]$$

wherein, in Equation 1 above,

λ_1 is a size of a long-axis vector E_l of the crystallite determined from image data obtained by a scanning ion microscope analysis of a cross-section of the positive electrode active material,

λ_2 is a size of a short-axis vector E_s of the crystallite determined from image data obtained by the scanning ion microscope analysis of the cross-section of the positive electrode active material, and

C_D above is an inner product value of a position unit vector P' and a long-axis vector E_l of the crystallite.

2. The positive electrode active material of claim 1, wherein the proportion (C1) of the plurality of crystallites C is 30% to 60% with respect to the total number of crystallites in the outer region.

3. The positive electrode active material of claim 1, wherein the proportion (C1) of the plurality of crystallites C to the total number of crystallites in the outer region is larger

than a proportion (C2) of the plurality of crystallites C to a total number of crystallites in the inner region.

4. The positive electrode active material of claim 3, wherein a difference between the proportion (C1) of the plurality of crystallites C to the total number of crystallites in the outer region and the proportion (C2) of the plurality of crystallites C to the total number of crystallites in the inner region is at least 3%.

5. The positive electrode active material of claim 1, further comprising:

a plurality of crystallites A wherein a crystallite long-axis orientation degree DoA is 0.5 to 1 and a crystallite c-axis orientation degree is 0.5 to 1;

a plurality of crystallites B wherein a crystallite long-axis orientation degree DoA is less than 0.5 and a crystallite c-axis orientation degree is 0.5 to 1; and

a plurality of crystallites D wherein a crystallite long-axis orientation degree DoA is less than 0.5 and a crystallite c-axis orientation degree is less than 0.5.

6. The positive electrode active material of claim 5, wherein the proportion (C1) of the plurality of crystallites C to the total number of crystallites in the outer region is larger than each of a proportion (A1) of the plurality of crystallites

A, a proportion (B1) of the plurality of crystallites B, and a proportion (D1) of the plurality of crystallites D.

7. The positive electrode active material of claim 5, wherein a proportion of the plurality of crystallites A to the total number of crystallites in the cross-section of the positive electrode active material is 5% to 40%, a proportion of the plurality of crystallites B is 5% to 40%, a proportion of the plurality of crystallites C is 20% to 80%, and a proportion of the plurality of crystallites D is 5% to 40%.

8. The positive electrode active material of claim 1, wherein the scanning ion microscope analysis is performed by obtaining a scanning ion microscope image by irradiating the cross-section of the positive electrode active material with a focused ion beam, then obtaining data segmented in a crystallite unit from the scanning ion microscope image using deep learning, and calculating DoA represented by Equation 1 above from the segmented data.

9. The positive electrode active material of claim 1, wherein the EBSD analysis is performed by obtaining EBSD Euler map data including position information and Euler angle information on each crystallite through EBSD measurement of the cross-section of the positive electrode active material, and calculating the c-axis rotation vector Rc (x, y, z) of the crystal lattice of the crystallite by means of Equation 2 below:

$$\begin{bmatrix} x \\ y \\ z \end{bmatrix} = R_z(\Psi)R_y(\Theta)R_x(\Phi) \begin{bmatrix} X \\ Y \\ Z \end{bmatrix} = \begin{bmatrix} \cos\Psi & -\sin\Psi & 0 \\ \sin\Psi & \cos\Psi & 0 \\ 0 & 0 & 1 \end{bmatrix} \begin{bmatrix} \cos\Theta & 0 & \sin\Theta \\ 0 & 1 & 0 \\ -\sin\Theta & 0 & \cos\Theta \end{bmatrix} \begin{bmatrix} 1 & 0 & 0 \\ 0 & \cos\Phi & -\sin\Phi \\ 0 & \sin\Phi & \cos\Phi \end{bmatrix} \begin{bmatrix} X \\ Y \\ Z \end{bmatrix} = \begin{bmatrix} \cos\Theta\cos\Psi & -\cos\Phi\sin\Psi + \sin\Phi\sin\Theta\cos\Psi & \sin\Phi\sin\Psi + \cos\Phi\sin\Theta\cos\Psi \\ \cos\Theta\sin\Psi & \cos\Phi\cos\Psi + \sin\Phi\sin\Theta\sin\Psi & -\sin\Phi\cos\Psi + \cos\Phi\sin\Theta\sin\Psi \\ -\sin\Theta & \sin\Phi\cos\Theta & \cos\Phi\cos\Theta \end{bmatrix} \begin{bmatrix} X \\ Y \\ Z \end{bmatrix} \tag{Equation 2}$$

wherein, [X, Y, Z] is (0, 0, 1), and Φ, θ, and Ψ each represent an Euler angle obtained from Euler map data.

10. The positive electrode active material of claim 1, wherein the positive electrode active material is a lithium composite transition metal oxide represented by Formula 1 below:



wherein, M¹ is at least one element selected from the group consisting of Mn and Al, M² is at least one element selected from the group consisting of W, Cu, Fe, V, Cr, Ti, Zr, Zn, Al, Ta, Y, In, La, Sr, Ga, Sc, Gd, Sm, Ca, Ce, Nb, Mg, B, and Mo, A is at least one element selected from the group consisting of F, Cl, Br, I, At, and S, and 0.98 ≤ x ≤ 1.20, 0 < a < 1, 0 < b < 1, 0 < c < 1, 0 ≤ d ≤ 0.2, and 0 ≤ y ≤ 0.2.

11. A positive electrode comprising the positive electrode active material claim 1.

12. A lithium secondary battery comprising the positive electrode of claim 11.

* * * * *